

## Validation of fluorescent-labeled microspheres for measurement of regional organ perfusion

ROBB W. GLENNY, SUSAN BERNARD, AND MICHAEL BRINKLEY

*Division of Pulmonary and Critical Care Medicine, Department of Medicine, University of Washington, Seattle, Washington 98196; and Molecular Probes Inc., Eugene, Oregon 97402*

GLENNY, ROBB W., SUSAN BERNARD, AND MICHAEL BRINKLEY. *Validation of fluorescent-labeled microspheres for measurement of regional organ perfusion.* J. Appl. Physiol. 74(5): 2585–2597, 1993.—Estimations of dog lung, pig heart, and pig kidney regional perfusion by use of fluorescent-labeled microspheres were compared with measurements obtained with standard radiolabeled microspheres. Pairs of radio- and fluorescent-labeled microspheres (15  $\mu\text{m}$  diam, 6 colors) were injected into a central vein of a supine anesthetized dog and the left ventricle of three supine anesthetized pigs while reference blood samples were simultaneously withdrawn from a femoral artery in the pigs. The lungs were cubed into  $\sim 2\text{ cm}^3$  pieces ( $n = 1,510$ ). Each pig heart and kidney was cubed into  $\sim 1\text{-g}$  pieces (total  $n = 192$  and  $120$ , respectively). The radioactivity of each organ piece and reference blood sample was determined using a scintillation counter with count rates corrected for decay, background, and spillover. Tissue samples and reference blood samples were digested with KOH and filtered and the fluorescent dye was extracted with a solvent, or the dye was extracted from lung tissue without filtering. The fluorescence of each sample was determined for each color by use of an automated spectrophotometer. Perfusion was calculated for each organ piece from both the radioactivity and fluorescence. Correlation between flow determined by radio- and fluorescent-labeled microspheres was as follows:  $r = 0.98 \pm 0.01$  (SD) (lung, filtered,  $n = 588$ ),  $r = 0.99 \pm 0.00$  (lung, nonfiltered,  $n = 710$ ),  $r = 0.95 \pm 0.02$  (heart, filtered), and  $r = 0.96 \pm 0.02$  (kidney, filtered). Compared with colored microspheres, methods for quantitating fluorescent-labeled microspheres are more sensitive, less labor intensive, and less expensive. Fluorescent-labeled microspheres provide a new nonradioactive method for single and repeated measurement of regional organ perfusion.

blood flow; pulmonary; heart; kidney

REGIONAL ORGAN PERFUSION can be estimated with hematogenously delivered microspheres (10, 15). When appropriately sized microspheres are used, regional blood flow is proportional to the number of microspheres trapped in the region of interest (3). Methods for quantitating the number of microspheres per region depend on the label attached to the microsphere, the most common being the measurement of radioactivity from radiolabeled microspheres. However, because of the radioactivity, these microspheres pose health risks, require special

precautions for use and disposal, have limited shelf lives, and consequently are relatively expensive. Recently, Hale et al. (8) and Kowallik et al. (13) reported the use of colored microspheres and, using heavy metal-labeled microspheres for measuring regional myocardial perfusion, Mori et al. (14) developed an X-ray fluorescence technique, obviating the need for radioactivity. Quantification of these microspheres requires tissue digestion and manual counting with a microscope (8), a computer-automated optical system, a spectrophotometer (13), or an X-ray fluorescence system (14). Whereas these methods have proven to be quite accurate compared with radiolabeled microsphere methods, they are relatively labor intensive.

The primary purpose of this study was to validate the use of fluorescent-labeled microspheres and automated fluorescent measurement for estimating regional organ perfusion. Although fluorescent-labeled microspheres have been used previously (6, 9, 11, 12), these studies used light microscopy and manual counting techniques to identify regions of ischemia or to estimate regional perfusion. Two secondary purposes of this study were to determine optimal fluorescent dye extraction methods and to evaluate two different types of sample readers: a cuvette reader, which measures the fluorescence of a single sample at a time, and a 96-well microplate reader. The results of our experiments and evaluations allow us to present a new method to quantitate regional tissue deposition of different fluorescent-labeled microspheres by use of automated fluorescence spectrophotometry.

### METHODS

#### *Evaluation of Fluorescent Technology*

**Fluorescent-labeled microspheres.** Fluorescent-labeled polystyrene microspheres, nominally 15  $\mu\text{m}$  diam, in seven colors (Table 1) were obtained from Molecular Probes (Eugene, OR). The fluorescent-labeled microspheres were shipped in 1 ml of distilled water and 0.01% Tween 80. These microspheres readily dissolved with xylenes or Cellosolve acetate (2-ethoxyethyl acetate, Aldrich Chemical, Milwaukee, WI), releasing the fluorescent dye into the solvent.

TABLE 1. *Excitation and emission wavelengths of available fluorescent-labeled microspheres in Cellosolve acetate*

Color	Excitation Wavelength, nm	Emission Wavelength, nm
Blue	360	420
Blue-green	430	457
Green	450	488
Yellow-green	490	506
Orange	530	552
Red	565	598
Crimson	600	635

We evaluated the feasibility of fluorescence spectrophotometry for measuring regional organ perfusion on the basis of the following criteria: 1) the fluorescent signal had to be linearly proportional to the dye concentration, 2) signals from multiple fluorescent colors had to be easily distinguished, 3) the fluorescent dye from tissue samples had to be easily recovered, and 4) enough fluorescent dye had to be delivered to the tissue sample to produce an adequate signal. We used a Perkin-Elmer LS-50 luminescence spectrophotometer (Beaconsfield, Buckinghamshire, UK) with excitation wavelength range 200–800 nm and emission wavelength range 200–900 nm. The machine was equipped with a pulsed xenon light source, variable excitation and emission monochrometers with variable slit widths, a red-sensitive photomultiplier tube (wavelength range 200–900 nm), a cuvette reader, and a 96-well microplate reader. All fluorescent measurements were made with excitation and emission slit widths of 4 nm and an emission filter blocking all light below 350 nm. A schematic representation of a fluorescent spectrophotometer is shown in Fig. 1.

Fluorescence occurs when a molecule absorbs energy

at a specific excitation wavelength and immediately releases the energy in the form of light at a specific emission wavelength (7). The difference between the optimal excitation and emission wavelengths is constant and termed the Stokes shift. We confirmed the optimal excitation and emission wavelengths for each fluorescent dye by dissolving fluorescent-labeled microspheres in Cellosolve acetate and then determining the fluorescent signal for various excitation and emission wavelengths until a maximal signal was obtained (Table 1, Fig. 2). It is important to note that the optimum excitation and emission wavelengths are affected by the choice of solvent and impurities in solution (7). The intensity of the fluorescent signal is also dependent on the excitation and emission slit widths.

The intensity of the emitted light,  $F$ , is described by the relationship

$$F = \phi I_0 (1 - e^{-\epsilon bc}) \quad (1)$$

where  $\phi$  is the quantum efficiency,  $I_0$  is the incident radiant power,  $\epsilon$  is the molar absorptivity,  $b$  is the path length of the cell, and  $c$  is the molar concentration of the fluorescent dye (7). For a constant  $\phi$ ,  $I_0$ ,  $\epsilon$ , and  $b$ , the relationship between the fluorescent signal and dye concentration should be linear for dilute dye concentrations (7). At high dye concentrations or short path lengths, the fluorescence intensity reaches a plateau as a result of "quenching." Quenching occurs because the exciting light is absorbed and cannot excite the entire sample (7).

Fluorescent colors are easily separable, because each color has a unique and narrow excitation spectrum. When excited at a specific wavelength, little "spillover" occurs from the emission from one color into the emission spectrum of an adjacent color. This selectivity can be further enhanced by narrowing the slit width of the

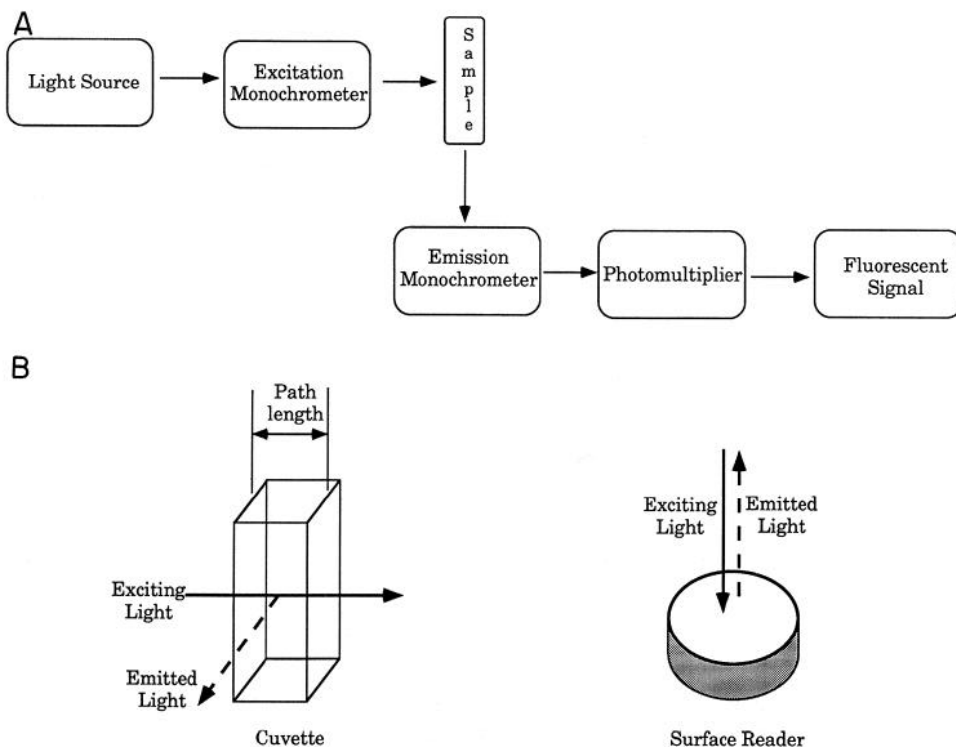


FIG. 1. A: schematic representation of a fluorescent spectrophotometer. Excitation and emission monochrometers are variable band-pass filters. B: 2 methods of measuring fluorescence. Cuvette reader excites sample over entire path length and reads emitted light at right angles. Surface reader excites sample from the top and reads emitted light returning along the same path direction.

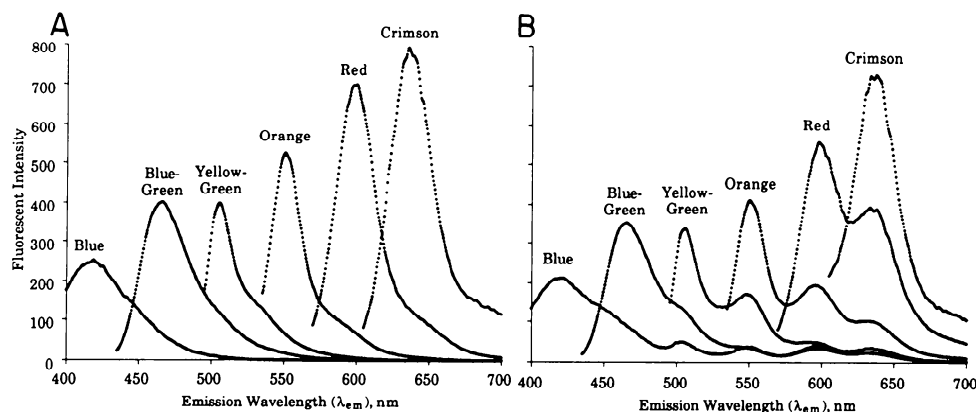


FIG. 2. Fluorescent emission spectra. A: composite graph of individual emission spectra of 6 colors excited at their optimal wavelength (Table 2). Fluorescence intensity increases through color spectrum from blue to crimson because of our red-sensitive photomultiplier tube, which was most efficient near red wavelengths. B: composite graph of 6 emission spectra from a sample containing all 6 colors. Because each emission spectrum is obtained by excitation at optimal wavelength, only 1 curve is generated each time sample is excited. If only peak intensity of emission spectrum is measured, relative fluorescence intensities of each color are similar whether read in pure samples or in samples with mixtures of colors.

emission monochromator so that only emitted light within a narrow spectral range is measured. Measurement of multiple fluorescent colors within a sample can be accomplished by reading the sample multiple times with specific matched excitation and emission wavelength filters for each color (Fig. 2). We evaluated the spillover of the fluorescent signal into the emission spectra of adjacent colors by measuring the fluorescent intensities of pure "standards" at each excitation/emission pair. A spillover matrix, representing the quantity of the signal from a specific fluorescent color in each color band, was constructed.

The optimal excitation and emission slit widths were evaluated by measuring the fluorescence intensities of pure samples at different slit width pairs and constructing spillover matrices. The excitation/emission slit widths used were 2.5/2.5, 2.5/4, 2.5/6, 2.5/8, 4/2.5, 4/4, 4/6, 4/8, 6/2.5, 6/4, 6/6, 6/8, 8/2.5, 8/4, 8/6, and 8/8 nm.

We evaluated the linearity and precision of the fluorescent signal with respect to the dye concentration and determined the fluorescence intensity as a function of the number of microspheres in the following manner. The number of fluorescent-labeled microspheres per volume of stock solution was determined by making a dilute solution of microspheres and manually counting them with a hemocytometer counting chamber. A known number of microspheres of each color was dissolved in Cello-solve acetate. Nine serial dilutions of each solution were made, and the intensity of the fluorescent signal was measured at each dilution with use of both the cuvette reader and the 96-well microplate reader. The precision of the fluorescent signal was evaluated by reading each sample from the serial dilutions 10 times.

The stability of the dyes in solvent was evaluated by dissolving fluorescent-labeled microspheres in Cello-solve acetate and reading the fluorescent intensities of each color on 7 consecutive days.

The fluorescence of the solvents, blood, and organ tissue without fluorescent-labeled microspheres was measured for intrinsic fluorescence.

Two types of sample readers were evaluated. Glass cuvettes with a path length of 10 mm and a volume of 0.7 ml were used to read sample fluorescence one sample at a time. The fluorescent signal in a cuvette reader was generated by exciting the sample along its entire path length

with the emitted light read at a right angle to the exciting light (Fig. 1). Samples were also read by a 96-well microplate reader. This attachment mechanically positioned an optical head above each well, exciting the sample within the well and reading the emitted light from the surface of the well (Fig. 1). The excited and emitted light was carried to and from the attachment by fiber-optic bundles attached to the spectrophotometer. Opaque polypropylene 96-microwell plates were obtained from Wilks Precision Instrument (Rockville, MD).

#### Comparison of Fluorescent-Labeled With Radiolabeled Microspheres

*Physical properties of fluorescent-labeled microspheres.* The diameters of the fluorescent-labeled microspheres were measured using scanning electron microscopy. The diameter variability of the fluorescent-labeled microspheres was determined with a Becton-Dickinson fluorescent-activated cell sorter (FACS analyzer). The densities of the fluorescent-labeled microspheres were estimated using microspheres of known densities (Pharmacia, Uppsala, Sweden) and gradient centrifugation in Percoll solution (Aldrich Chemical). The uniformity of fluorescence intensity was examined with the FACS analyzer.

*Radiolabeled microspheres.* Radioactive  $15.5 \pm 0.1$ - $\mu$ m-diam styrene-divinyl benzene microspheres with five radiolabels ( $^{141}\text{Ce}$ ,  $^{113}\text{Sn}$ ,  $^{103}\text{Ru}$ ,  $^{95}\text{Nb}$ , and  $^{46}\text{Sc}$ ) were obtained from Dupont (NEN Research Products, Boston, MA) and suspended in 10% dextran with 0.02% Tween. The reported density of these microspheres was 1.4 g/ml.

*Regional pulmonary perfusion study.* A 27-kg male dog was initially anesthetized with thiamyl sodium (15 mg/kg iv) and maintained with a combination of intravenous ketamine hydrochloride (3.3 mg/kg), valium (0.1 mg/kg), and pentobarbital sodium (3.0 mg/kg) given every 15–20 min. The animal was supine and mechanically ventilated at a rate and tidal volume to maintain a  $\text{PCO}_2$  of  $\sim 35$  Torr. Femoral venous, pulmonary arterial, and femoral arterial catheters were placed. Hemodynamics and arterial blood gases were monitored throughout. Before injection, the radio- and fluorescent-labeled microspheres were sonicated, vortexed, and combined in a single syringe. Five different pairs of radio- and fluorescent-labeled microspheres were injected via a femoral catheter

every 20 min. The last injection had two fluorescent colors with a single radiolabeled microsphere. At least  $4 \times 10^6$  radiolabeled microspheres were used for each injection to ensure that adequate numbers of microspheres were present in each lung piece (5). The number of fluorescent microspheres needed in each tissue sample to produce an adequate fluorescent signal was determined from preliminary experiments, as described above. Approximately  $4 \times 10^6$  blue,  $3 \times 10^6$  yellow-green,  $4 \times 10^6$  green,  $4 \times 10^6$  orange,  $5 \times 10^6$  red, and  $4 \times 10^6$  crimson microspheres were injected. Each injection ( $\sim 30$  ml vol) was performed over four to five respiratory cycles and was followed by a saline flush.

The animal was then deeply anesthetized, heparinized, exsanguinated, and killed by injection of intravenous pentobarbital sodium (150 mg/kg). A sternotomy was performed, large-bore catheters were placed into the pulmonary artery and left atrium, and the aorta was tied off. The lungs were perfused with normal saline until clear of blood, removed from the chest, and allowed to dry on continuous positive airway pressure of 25 cmH<sub>2</sub>O.

When dry, the lungs were suspended vertically in a plastic-lined square box and embedded in rapidly setting urethan foam (2 lb Polyol and Isocyanate, International Sales, Seattle, WA). The foam block was cut into uniformly sized cubes,  $\sim 1.9$  cm<sup>3</sup> in volume, resulting in 1,510 pieces. Any foam adherent to lung pieces was removed. Regional perfusion to each lung piece was determined by radioactivity and fluorescence, as described below.

*Regional myocardial, renal, and relative blood flow study.* Three pigs ( $16.5 \pm 2.6$  kg) were chemically restrained with ketamine (20 mg/kg) and xylazine (2 mg/kg). Two of the animals were anesthetized with a combination of intravenous ketamine hydrochloride (3.3 mg/kg), valium (0.1 mg/kg), and pentobarbital sodium (3.0 mg/kg) every 15–20 min. Anesthesia was induced in the third animal with pentobarbital sodium (22 mg/kg), and a single dose of Pavulon (0.2 mg/kg) was given to produce paralysis. Anesthesia was maintained with pentobarbital sodium (5.5 mg/kg) every 20–30 min. The animals were supine and mechanically ventilated at a rate and tidal volume to maintain a PCO<sub>2</sub> of  $\sim 35$ –45 Torr. Femoral venous, pulmonary arterial, and two femoral arterial catheters were placed in each animal. Before injection, the radio- and fluorescent-labeled microspheres were sonicated, vortexed, and combined in a single syringe ( $\sim 15$ –20 ml vol). Simultaneous injections of three isotopes of radiolabeled microspheres (<sup>141</sup>Ce,  $3.5 \times 10^6$ ; <sup>113</sup>Sn,  $4.4 \times 10^6$ ; and <sup>103</sup>Ru,  $3.3 \times 10^6$ ) and two colors of fluorescent-labeled microspheres (yellow-green,  $4.0 \times 10^6$ ; crimson,  $4.0 \times 10^6$ ) were injected via left ventricular catheters that had been placed in a retrograde manner across the aortic valve. The injections were performed over 45 s and were followed by saline flushes. During the microsphere injection, blood was sampled from each femoral arterial catheter by use of heparinized glass syringes and a dual-piston Harvard withdrawal pump at a rate of 10 ml/min. Blood was withdrawn from the animals until their cardiac outputs were  $\sim 50\%$  of their baseline outputs. A second set of simultaneous left ventricular injections of two isotopes of radiolabeled microspheres (<sup>95</sup>Nb,

$4.7 \times 10^6$ ; <sup>46</sup>Sc,  $3.9 \times 10^6$ ) and a single color of fluorescent-labeled microspheres (orange,  $4.0 \times 10^6$ ) was performed. Reference femoral artery blood samples were obtained during this injection as well.

After completion of the study, the animals were killed by injection of intravenous pentobarbital sodium (150 mg/kg), and the heart and kidneys were removed. Each heart was cut into  $\sim 1$ -g pieces ( $0.80 \pm 0.37$  g, total  $n = 192$ ), and the kidneys were cut into  $\sim 1$ -g pieces ( $1.07 \pm 0.44$  g, total  $n = 120$ ). The radioactivity and fluorescence of each tissue piece and the reference blood samples were determined by methods described below.

*Radiolabel-determined perfusion.* The radioactivity in each organ piece and reference blood sample was determined using a  $3 \times 3.25$ -in. sodium well crystal gamma counter (Minaxi gamma counting system, model 5550, Packard, Downers Grove, IL). Each sample was corrected for decay time, background counts, and spillover by use of the matrix inversion method (16). Pure isotope samples were used to select one energy window per isotope, such that  $\geq 90\%$  of the principal peak was included and none of the energy windows overlapped. The spillover matrix was calculated from these samples by use of the previously defined energy windows. Each tissue piece was counted long enough to ensure a counting error of  $< 1\%$ .

Relative microsphere-determined blood flow for each lung region, isotope, and color was calculated by dividing the measured radioactivity or fluorescence in each piece by the mean radioactivity or fluorescence for all pieces. The microsphere-determined regional myocardial and renal perfusion was calculated by the standard reference flow technique (15)

$$\text{regional perfusion}_i = \frac{(\text{sample}_i \text{ measurement}) \times (\text{reference blood withdrawal rate})}{\text{reference blood measurement}} \quad (2)$$

where the measurement is either radioactivity or fluorescence intensity and  $i$  denotes the  $i$ th sample.

*Fluorescence method 1: tissue digestion and microsphere recovery by filtration.* The heart and kidney pieces from the three pigs and one-half of the lung pieces were individually digested in 7 ml of 4 M KOH and 2% Tween 80. The tissue pieces were completely digested within 24 h and did not require agitation, because warm KOH was used. The digested tissue pieces were then individually filtered through 10- $\mu$ m-pore polycarbonate filters (Poretics, Livermore, CA) by use of negative pressure. The vials and filtering burette were washed twice with 2.0% Tween, and the wash was filtered to recover residual microspheres. The filter and filtered material from each organ piece were placed in individual polypropylene test tubes, and 1.25 ml of Cellosolve acetate were added to each tube by use of a calibrated pipette (Eppendorf Repeater Pipet, Brinkmann, precision  $< 0.05$ – $0.1\%$ ) to extract the fluorescent dye. Identical volumes of solvent were necessary so that the relationship between extracted dye concentration and the number of microspheres in each tissue piece would be linear. After  $\geq 4$  and up to 24 h, a sample of dye/solvent from each organ piece was pipetted into a glass cuvette (0.7 ml vol, 10 mm path

length) and the fluorescence of each color was determined. The excitation and emission wavelengths were set manually at the beginning of each study with all samples measured at the specified wavelengths. Because of bookkeeping errors unrelated to the fluorescence methods, 212 lung pieces could not be processed. These samples were not read in the spectrophotometer, resulting in only 588 lung pieces being used in the analysis. Because these pieces were selected without bias, their exclusion should not have influenced the statistical results. Each heart and kidney sample of dye/solvent was also pipetted into individual wells of 96-well microplates.

The reference blood samples were processed in a similar fashion. Each sample was rinsed with 20 ml of 2% Tween, and then ~2 ml of 16 M KOH were added. After 24 h, the reference blood samples were filtered, and the retained microspheres were dissolved in Cellosolve acetate, as described previously for the individual tissue pieces.

The fluorescence of each dye/solvent sample was measured at the excitation/emission wavelength pairs in Table 2, with slit widths of 4 nm. The fluorescence of each sample was read individually in a glass cuvette as well as in batches by means of a 96-well microplate reader.

*Fluorescence method 2: dye extraction without filtration.* The remaining lung pieces ( $n = 710$ ) were placed in individual polypropylene test tubes, and 1.25 ml of Cellosolve acetate were added to each tube by use of a calibrated pipette. After it was soaked in the solvent for  $\geq 24$  h, a sample of dye/solvent was pipetted into a glass cuvette and into individual wells of 96-well microplates. The fluorescence of each dye/solvent sample was measured at the excitation/emission wavelength pairs in Table 2. Slit widths of 4 nm were used for all measurements. The fluorescence of each sample was read individually in glass cuvettes as well as in batches by means of a 96-well microplate reader (only 462 lung pieces were read in the microplate reader).

### Statistics

Flows determined by radio- and fluorescent-labeled microsphere techniques were compared using least-squares linear regression. The linear relationship between each pair of radio- and fluorescent-labeled microspheres was determined separately for each color and injection. The slopes and intercepts were compared with unity and the

origin, respectively. The linear correlation coefficient expressed the strength of the linear relationship between the radio- and fluorescent-labeled microsphere estimates of regional perfusion. The standard error of the estimate (SEE) was determined for each linear and quadratic regression to provide a measure of random error (17). Fluorescent- and radiolabeled flow measurements were compared by the method of Bland and Altman (4) using the percent difference between measurements. All values are expressed as means  $\pm$  SD. The variability in microsphere diameters, microsphere fluorescence, and repeated measurement of fluorescent signals was quantified by the coefficient of variation ( $CV = 100 \cdot SD/\text{mean}$ ).

## RESULTS

### *Evaluation of Fluorescent Technology*

The "spillover matrix" from pure samples of each fluorescent color is presented in Table 2. The only colors with a significant amount of spillover into adjacent color bands were blue-green (18.1% into green) and green (8% into blue-green and 8.8% into yellow-green). None of the colors spilled over into bands beyond immediately adjacent colors. The spillover matrix was similar for the 96-well microplate reader, except for the green, which had a relative signal in the blue-green band of 22.9%, and the yellow-green, which had a relative signal in the green band of 20.9%.

The fluorescence signals obtained from the pure samples changed greatly, with small changes in the emission slit width but was unaffected by changes in the excitation slit width. The fluorescence intensity of a given color increased by 20–22 times as the emission slit width increased from 2.5 to 8 nm, while the fluorescence intensity increased by only 10% as the excitation slit width increased over the same range. The spillover matrices were similar for all excitation/emission slit width pairs. The signal-to-noise ratio, as defined by the fluorescence intensity of a color at its optimal excitation/emission wavelength pair divided by background fluorescence, was constant for all excitation/emission slit width pairs.

The fluorescence intensity as a function of microsphere number for each color is shown in Fig. 3. When read in cuvettes, the fluorescent signal was nearly linear with respect to the number of microspheres over the range of 25–16,000 microspheres/sample. Although each color had a slight curvature, as expected from Eq. 1, the linear correlation coefficients ( $r$ ) were  $>0.99$  for all colors, with the SEE ranging from 5.6 to 47.89 for orange and crimson, respectively. Hence, despite the slight non-linearity, 98% of the variability in the fluorescence intensity was explained by a linear relationship to the number of microspheres in the sample. The fluorescence intensity per microsphere (slope of the linear relationship) increased through the color spectrum from blue to crimson, because our red-sensitive photomultiplier tube was most efficient near red wavelengths.

The curvilinear relationship between fluorescent intensity and microsphere number was dependent on the range of microsphere numbers. Over the maximum range of microsphere numbers (50–16,000 microspheres/sample), the relationship between fluorescent intensity and

TABLE 2. Spillover matrix of fluorescent colors

Color	Color Bands						
	Blue	Blue-green	Green	Yellow-green	Orange	Red	Crimson
Blue	100.0	0.0	0.0	0.0	0.0	0.0	0.0
Blue-green	0.2	100.0	18.1	0.0	0.0	0.0	0.0
Green	0.0	8.0	100.0	8.8	0.0	0.0	0.0
Yellow-green	0.0	0.0	1.5	100.0	0.0	0.0	0.0
Orange	0.0	0.0	0.0	0.1	100.0	0.3	0.0
Red	0.0	0.0	0.0	0.0	0.2	100.0	3.3
Crimson	0.0	0.0	0.0	0.0	0.0	2.6	100.0

Values represent amount of a given color's signal in each color band and are relative to an arbitrary value of 100 for the color signal within its own color band.

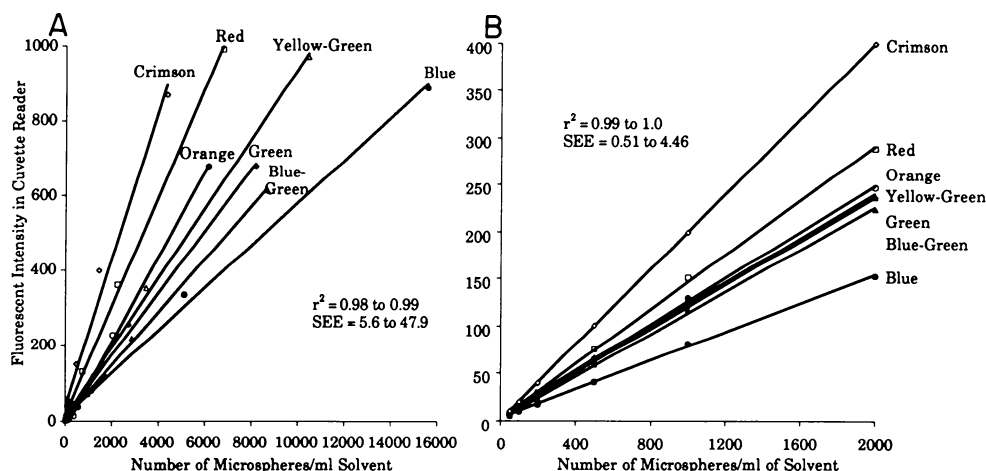


FIG. 3. Fluorescence intensity as a function of no. of microspheres per sample. Each sample was read in a cuvette with excitation and emission slit widths of 4 nm. A: relationship between fluorescence intensity and no. of microspheres is nearly linear over a broad range of microspheres. Although there was a slight curvature, as expected from Eq. 1, 98% of variability in fluorescence intensity was explained by a linear fit to no. of microspheres in sample. Fluorescence intensity per microsphere (slope of linear relationship) increased through color spectrum from blue to crimson, because our red-sensitive photomultiplier tube was most efficient near red wavelengths. B: same plot as A over a narrower range of microspheres. Relationship between fluorescence intensity and no. of microspheres remains linear. Curvature is less of a problem at lower dye concentrations.

microsphere number was more accurately characterized by a quadratic function. When a quadratic function was used, the SEE of the serial dilutions as a function of microsphere number improved significantly, ranging from 1.50 to 3.52. When the range of microsphere numbers was restricted to those usually used for regional perfusion studies (50–2,000 microspheres/sample), the relationship between fluorescent intensity and microsphere number was more linear (Fig. 3A), with  $r > 0.999$  for all colors and  $SEE = 0.51$ –4.46. When a quadratic function was fit to the fluorescent intensity as a function of microsphere number for this narrow range of microspheres, the SEE was again slightly smaller (0.19–1.56).

As with radiolabeled microspheres, the accuracy of the fluorescent-labeled microsphere method at low flow states will be primarily dependent on Poisson statistics rather than the signal from the microspheres. The accuracy of the signal from relatively few microspheres (50/sample) is quite good (Fig. 3B).

The precision of the fluorescent signal, as quantified by the CV for repeated measurements of the same sample, had a Gaussian distribution and ranged from 0.2 to 1.7% for each color and dilution (both cuvette and 96-well microplate reader). The slope of a line characterizing the intensity of each color as a function of days was not significantly different from zero, indicating that each color remained stable in Cellosolve acetate for  $\leq 7$  days. The CV of the fluorescent signal for each color ranged from 1.7 to 4.3% when read in cuvettes each day over 7 days.

Cellosolve acetate and xylenes had no intrinsic fluorescence. Lung tissue (without fluorescent microspheres) soaked in Cellosolve acetate did not produce any measurable fluorescence. Heart and kidney tissue (without fluorescent microspheres) digested with KOH and filtered did not leave any fluorescent material on the filter.

#### Comparison of Fluorescent-Labeled and Radiolabeled Microspheres

**Physical properties of fluorescent microspheres.** The fluorescent-labeled microspheres measured 14.7  $\mu\text{m}$  diam

with a CV of 2.1%. Their density was 1.02 g/ml. The CV in fluorescence intensity per microsphere ranged from 3.4 to 9.4%, except for the blue-green microspheres, which had a fluorescent variability of 22.8%.

**Regional pulmonary perfusion study.** The dog's hemodynamics and arterial blood gases remained stable throughout the study and were not affected by microsphere injections.

The linear relationships between radio- and fluorescent-labeled regional perfusion estimates are presented in Tables 3 and 4 and shown in Fig. 4 for a single paired injection. Both the filtering and nonfiltering methods produced highly correlated linear relationships among paired injections. A quadratic fit to the relationship between radio- and fluorescent-labeled regional perfusion estimates resulted in intercepts that were not significantly different from the origin (except for orange, soaked method) but did not appreciably change the SEE for any of the colors. The relationship between the two simultaneously injected fluorescent-labeled microspheres was also highly correlated ( $r = 0.99$ , filtered and nonfiltered methods).

**Regional myocardial, renal, and relative blood flow study.** The pigs' hemodynamics and arterial blood gases remained stable throughout the initial part of the stud-

TABLE 3. Fluorescence method 1: filtered samples read in cuvettes

Radiolabel	Fluorescent Label	$r$	Slope	Intercept	SEE
$^{141}\text{Ce}$	Blue	0.98	0.97*	0.04†	0.12
$^{113}\text{Sn}$	Crimson	0.99	1.09*	-0.09†	0.19
$^{103}\text{Ru}$	Yellow-green	0.98	1.02*	-0.02	0.15
$^{95}\text{Nb}$	Orange	0.98	1.00	0.00	0.14
$^{46}\text{Sc}$	Red	0.98	1.02	-0.02	0.15
$^{46}\text{Sc}$	Green	0.98	0.99	0.01	0.14
Mean $\pm$ SD		0.98 $\pm$ 0.01	1.01 $\pm$ 0.04	-0.01 $\pm$ 0.04	0.15 $\pm$ 0.02

Values represent radio- vs. fluorescent-labeled estimates of pulmonary perfusion ( $n = 588$  pieces). SEE, standard error of estimate;  $r$ , correlation coefficient. \* Statistically different from 1.0 ( $P < 0.05$ ). † Statistically different from 0.0 ( $P < 0.05$ ).



TABLE 4. Fluorescence method 2: nonfiltered samples read in cuvettes

Radiolabel	Fluorescent Label	r	Slope	Intercept	SEE
<sup>141</sup> Ce	Blue	0.99	0.95*	0.05†	0.08
<sup>113</sup> Sn	Crimson	0.99	1.00	-0.01	0.10
<sup>103</sup> Ru	Yellow-green	0.99	1.00	0.00	0.11
<sup>95</sup> Nb	Orange	0.99	0.98*	0.02	0.10
<sup>46</sup> Sc	Red	0.99	0.98*	0.04†	0.09
<sup>46</sup> Sc	Green	0.99	0.98*	0.02	0.09
Mean ± SD		0.99±0.00	0.98±0.02	0.02±0.02	0.09±0.01

Values represent radio- vs. fluorescent-labeled estimates of pulmonary perfusion ( $n = 710$  pieces). \* Statistically different from 1.0 ( $P < 0.05$ ). † Statistically different from 0.0 ( $P < 0.05$ ).

ies. After blood removal, cardiac outputs and mean arterial pressures decreased by ~50%. In two pigs, blood pressures were not affected by microsphere injections, whereas in the third pig, there was a transient decrease of 10 mmHg in mean arterial pressure 5 min after microsphere injection.

The linear relationships between radio- and fluorescent-labeled regional perfusion estimates for heart and kidney are presented in Table 5 and shown for myocardial perfusion in Fig. 5 for a single paired injection. Filtering methods produced highly correlated linear relationships among paired injections. The relationship between simultaneously injected fluorescent-labeled microspheres was also highly correlated.

**Evaluation of 96-well microplate reader.** The fluorescence intensity as a function of microsphere number for each color read with the 96-well microplate reader is shown in Fig. 6. Compared with the cuvette reader, the fluorescent signal from the microplate reader was linear over a shorter range of microspheres, plateauing early because of quenching. Quenching likely occurred with the well microplate reader, because it was a surface reading instrument with a relatively short path length (see Eq. 1). The quenching artifact can be minimized by restricting the fluorescent signals to the linear range (more dilute concentrations, Fig. 6A). When the range of microsphere numbers was restricted to those usually used for regional perfusion studies (50–2,000 microspheres/sample), the relationship between fluorescent intensity and

microsphere number was more linear (Fig. 6A), with  $r > 0.995$  for all colors and  $SEE = 1.12$ – $7.42$ . When a quadratic function was fit to the fluorescent intensity as a function of microsphere number for this narrow range of microspheres, the SEE was again slightly smaller (0.08–2.55). In general, except for blue, all the colors produced an adequate signal in the microplate reader. The blue signal was less intense because of decreased fiber-optic transmission efficiency within the blue light range and the red-sensitive photomultiplier tube used in our instrument.

The sensitivity of the microplate reader was slightly less than that of the cuvette reader. Fluorescent signals from each lung piece (soaked method) were obtained by both the microplate and cuvette readers. When these values were plotted against each other, the sensitivity of the microplate reader compared with that of the cuvette reader was quantitated by the slope of the relationship. The relative sensitivities for each color were as follows: blue = 7%, green = 74%, yellow-green = 79%, orange = 64%, red = 64%, and crimson = 86%.

Figure 7 compares the regional perfusion estimated from fluorescent- and radiolabeled microspheres with use of the microplate reader to obtain the fluorescent intensities. Despite the slight curvature of the relationship, a linear fit to the data explains 93–96% of the variability in regional pulmonary perfusion (Table 6). The poorest linear fits, slopes less than unity and intercepts greater than the origin, were shown for those colors (orange and red) with fluorescent intensities greater than the linear range of the microplate reader.

The relationship between cuvette and microplate reader fluorescent intensities is curvilinear and can be characterized by a second-degree polynomial. If this relationship remains constant over experiments, the quenching artifact can be mathematically corrected. When the orange and red intensities were mathematically corrected for quenching, the linear relationship between fluorescent- and radiolabeled regional perfusion estimates improved, resulting in slopes of 0.97 and 0.96 and intercepts of 0.07 and 0.07 for orange and red, respectively.

Regional myocardial and renal perfusion estimates by use of fluorescent-labeled microspheres and read in the

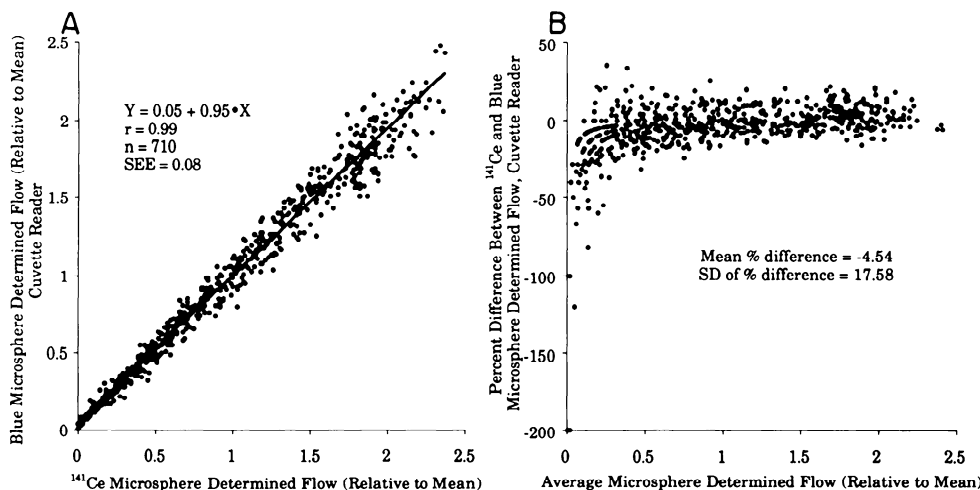


FIG. 4. Regional organ perfusion as determined by simultaneous injection of fluorescent- and radiolabeled microspheres. A: flow per lung piece, relative to mean. Six different fluorescent and 5 different radiolabeled microspheres were injected simultaneously. Plot is of 1 fluorescent- and radiolabeled microsphere pair, and each point represents 1 tissue piece. Fluorescent dye was extracted from these tissue pieces by soaking method and read in a cuvette. B: percent difference between regional pulmonary perfusion as measured by fluorescent- and radiolabeled microspheres as a function of flow per piece.

TABLE 5. Comparison of myocardial and renal perfusion estimates by use of different microsphere labels

Microsphere Label	Microsphere Label	Organ	r	Slope	Intercept	SEE
Radioactive	Fluorescent	Heart	0.95±0.02	1.08±0.11	-0.05±0.10	0.20±0.11
Radioactive	Fluorescent	Kidney	0.96±0.02	0.90±0.08*	0.15±0.06†	0.16±0.07
Fluorescent	Fluorescent	Heart	0.99±0.01	1.05±0.13	0.03±0.05	0.09±0.01
Fluorescent	Fluorescent	Kidney	0.99±0.01	1.02±0.13	0.00±0.07	0.10±0.01
Radioactive	Radioactive	Heart	1.00±0.00	1.00±0.03	0.02±0.02	0.05±0.01
Radioactive	Radioactive	Kidney	0.99±0.01	1.02±0.04	0.00±0.03	0.10±0.02

Values are means ± SD of 192 myocardial and 120 renal samples. Filtered samples were read in cuvettes. \* Statistically different from 1.0 ( $P < 0.05$ ). † Statistically different from 0.0 ( $P < 0.05$ ).

96-well microplate reader were not as good as those estimated from cuvette readings or when flow was estimated relative to the mean (Fig. 8, Table 7).

## DISCUSSION

The important findings of this study are that 1) fluorescent-labeled microspheres provide a nonradioactive method of accurately measuring regional tissue perfusion, 2) multiple colors can be easily separated, currently allowing up to seven measurements of perfusion in a single experiment, 3) fluorescence measurements are quite sensitive, 4) the methods are relatively simple, and 5) fluorescent microsphere techniques are relatively inexpensive compared with radiolabeled microspheres.

Initial methods for measuring regional organ flow used indicator-dilution techniques. The microsphere method is simply a modification of this technique, in which entrapment of the microspheres accomplishes the integration of the indicator-dilution technique (10). In order for the microspheres to accurately measure regional organ flow, certain criteria must be met: 1) the microspheres must be distributed evenly within the bloodstream, 2) the microspheres must be completely trapped, and 3) lodging of the microspheres in the capillary must have no effect on local perfusion. Because of the particulate nature of the microspheres, there has been some concern that microspheres may not faithfully represent blood flow distribution at the level of the capillaries (18). However, if the feeding vessels to the observed organ pieces are only a few times larger than the microspheres, regional flow

should be faithfully estimated by the microsphere technique (3).

Spectrophotometry provides a measure that is both linear with respect to the number of fluorescent-labeled microspheres per sample and has little variability. The linear correlation coefficient between fluorescence and number of microspheres was  $>0.99$  for all colors. This linear relationship held over the range of 25–16,000 microspheres/ml of solvent, indicating that both low and high flows are accurately measured. The measurement of fluorescence intensity is very precise. This is demonstrated by the small variability in intensity when the same sample is read multiple times within a few minutes. Although the variability in sample measurement increases when samples are read on consecutive days, the CV remains quite small.

The linear correlation between regional organ perfusion estimates by use of fluorescent- and radiolabeled microspheres was excellent. The slopes and intercepts of some comparisons were different from unity and the origin because of a systematic bias in the radioactive and/or fluorescent method. The differences from unity and the origin were quite small and were statistically different only because of the very tight linear fit and the slight curvature expected from the fluorescent intensity equation (Eq. 1). Fitting a quadratic function to the relationship between fluorescent- and radiolabeled perfusion estimates produced intercepts that were not significantly different from zero in all cases except one, suggesting that the small nonlinearity of the relationship is responsible for the nonzero intercepts. When the number of mi-

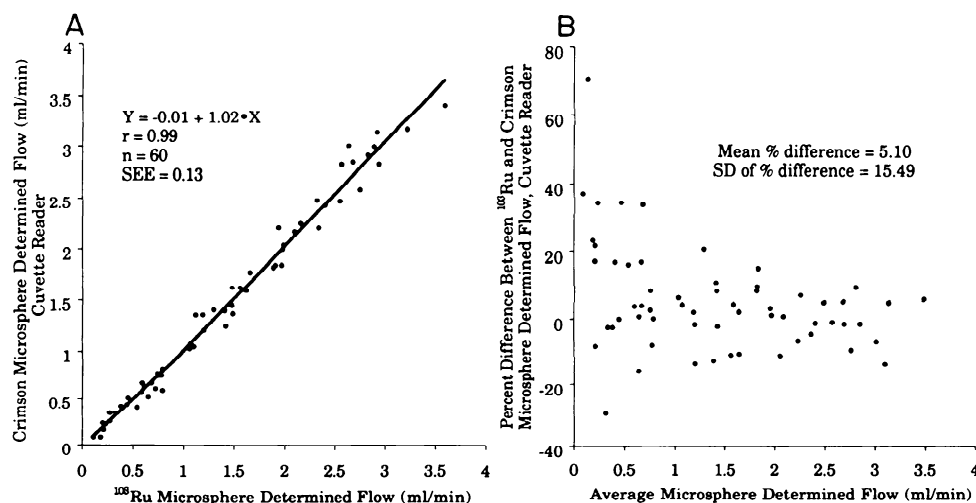


FIG. 5. Regional organ perfusion as determined by simultaneous injection of fluorescent- and radiolabeled microspheres. A: myocardial flow per piece by use of reference flow technique for 1 animal. Five different fluorescent and 3 different radiolabeled microspheres were injected simultaneously. Plot is of 1 fluorescent- and radiolabeled microsphere pair; each point represents 1 tissue piece. Fluorescent dye was extracted from these tissue pieces by filtration and read in a cuvette. B: percent difference between regional myocardial perfusion as measured by fluorescent- and radiolabeled microspheres as a function of flow per piece.



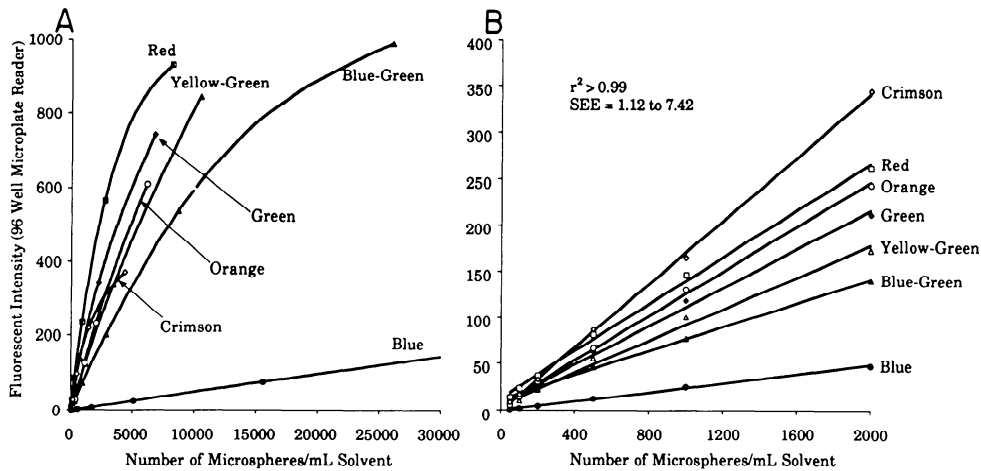


FIG. 6. Fluorescent intensity as a function of no. of microspheres per sample. Each sample was read in a microplate reader. A: relationship between fluorescence intensity and no. of microspheres was curvilinear as a result of quenching. B: same plot as A over a narrower range of microspheres. Relationship between fluorescence intensity and no. of microspheres is more linear for all colors.

microspheres used is restricted to those usually used for regional perfusion studies (50–2,000 microspheres/sample), the relationship between fluorescent intensity and microsphere number is essentially linear. If, however, this small nonlinearity is important, it can be mathematically corrected using a quadratic function determined from serial dilutions of standard microspheres. As a fluorescent spectrophotometer ages, the quadratic characterization of fluorescent intensity as a function of microsphere number may change and the quadratic relationship should be measured periodically. The observation that the SEE was not significantly different when a linear or quadratic function was fit to the relationship between fluorescent- and radiolabeled microsphere perfusion estimates suggests that most of the error arises from measurement as opposed to fitting a line to a curvilinear relationship.

The correlation between simultaneously measured regional perfusion was not perfect, indicating that there is a measurable, albeit small, error in estimating regional blood flow with microsphere techniques. A number of excellent studies have quantitated the sources of error when radiolabeled microsphere methods are used (1, 5, 19). Fluorescent-labeled microsphere methods share many of the same sources of error, including the Poisson nature of microsphere distribution and counting error. Although this study does not allow determination of

error sources or their relative contributions to the total error, the most likely sources are 1) loss of microspheres through filtering and sample handling, 2) unequal volumes of solvent added to each sample, and 3) the fluorescent measurement of each sample. The findings that the soaked lung samples provided the best correlation between the fluorescent- and radiolabeled methods and that all the outliers in the filtered samples had fluorescent intensities less than expected from the radioactivity suggest that microsphere loss is the most important source of error. Fluorescent measurement should be a relatively smaller source of error because of the excellent reproducibility in repeated measurements.

Fluorescence technology is superior to radioactive measurements in separating spectral signals. Because only the emission spectrum of one color is produced with excitement at the appropriate excitation wavelength, there is little spillover of one color's signal into another with use of fluorescent spectrophotometry. At present, there are seven fluorescent colors commercially available with excitation and emission spectra that allow them to be easily separated. Standard sodium iodide crystals can resolve the eight available radiolabels (2), and absorbance spectrophotometry is able to resolve five colors (13).

Because of the pairing of excitation and emission spectra, different color signals can be separated without having to solve systems of linear equations to account for

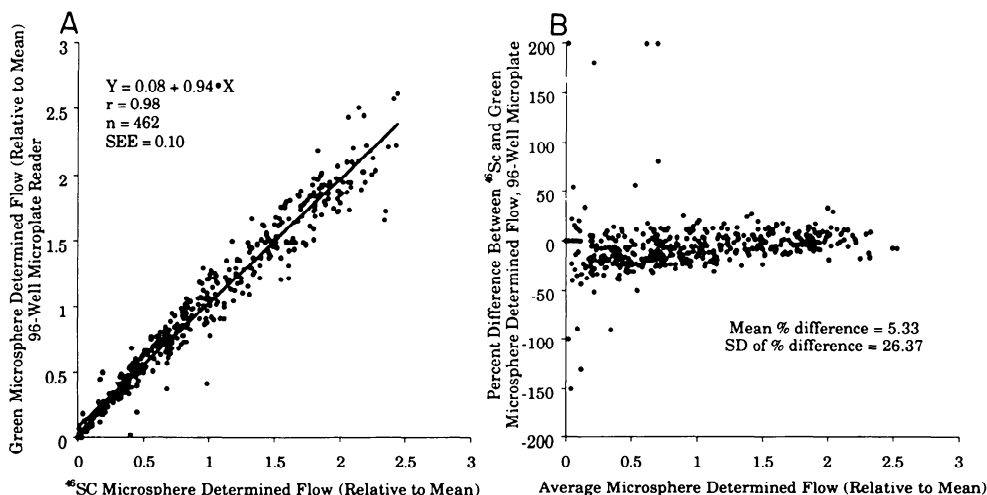


FIG. 7. Regional organ perfusion as determined by simultaneous injection of fluorescent- and radiolabeled microspheres. A: flow per lung piece, relative to mean. Six different fluorescent and 5 different radiolabeled microspheres were injected simultaneously. Plot is of 1 fluorescent- and radiolabeled microsphere pair; each point represents 1 tissue piece. Fluorescent dye was extracted from these tissue pieces by soaking and read in a microplate reader. B: percent difference between regional pulmonary perfusion as measured by fluorescent- and radiolabeled microspheres as a function of flow per piece.

TABLE 6. Fluorescence method 2: nonfiltered samples read in microplates

Radiolabel	Fluorescent Label	r	Slope	Intercept	SEE
<sup>141</sup> Ce	Blue	0.97	1.01	0.02†	0.21
<sup>113</sup> Sn	Crimson	0.97	0.95	0.08†	0.20
<sup>103</sup> Ru	Yellow-green	0.98	1.00	0.03†	0.17
<sup>95</sup> Nb	Orange	0.97	0.89*	0.13†	0.17
<sup>46</sup> Sc	Red	0.97	0.86*	0.16†	0.17
<sup>46</sup> Sc	Green	0.98	0.95*	0.08†	0.10
Mean ± SD		0.97±0.01	0.94±0.06	0.09±0.02	0.17±0.04

Values represent radio- vs. fluorescent-labeled estimates of pulmonary perfusion (*n* = 462 pieces). \* Statistically different from 1.0 (*P* < 0.05). † Statistically different from 0.0 (*P* < 0.05).

signal spillover. Both the radiolabel technique and the colored microsphere methods require corrections for signal spillover into adjacent spectral windows (13, 16). Although it is relatively simple to make these corrections, the algorithms to do so must either be purchased commercially or programmed by each investigator. The ability to resolve the separate fluorescent signals without having to correct for spillover also removes one more potential source of error in data collection (2, 19). Although all seven colors used in this study can be used simultaneously, green is less desirable because of its spillover into adjacent color bands. Although green may not be a good color to use in conjunction with blue-green or yellow-green, it can still be used with all the other colors.

Two potential problems arise from the emission spectra of one color overlapping the excitation spectra of an adjacent color. If the light used to excite one color excites an adjacent color, light from the second color will also be emitted and could contribute to the total signal of the first color if there is sufficient emission overlap between the two colors. Six of the seven colors used in this study have sufficient separation between their respective excitation and emission spectra, so that when the emission slit is positioned properly and the slit width is correctly adjusted, only the desired color is excited (Table 2). The second potential problem is that the emitted light from the initially excited color will be partially absorbed by other dye molecules in the solution (self-absorption),

thereby broadening and decreasing the measured fluorescent signal from the first color. This problem occurs only if the total dye concentrations are greater than ~1 μM, a concentration corresponding to >1 × 10<sup>5</sup> microspheres/ml of solvent.

The sensitivity of the fluorescent methods is dependent on the amount of dye per microsphere, the quantum efficiency of the fluorescent dye (*Eq. 1*), the optics of the spectrophotometer, and the spectrophotometer parameters used for measuring the fluorescent signal. The fluorescent-labeled microspheres used in this study had been maximally loaded with dye to provide as large a fluorescent signal as possible. The quantum efficiency (ratio of emitted light to absorbed light) of the fluorescent dyes was high, ranging from 0.75 to 0.90 for each of the dyes except crimson, which had a quantum efficiency of 0.45. Because crimson produced the strongest fluorescent signal per microsphere (Figs. 2 and 3), the relatively low quantum efficiency of crimson must have been offset by greater loading of this color into the microspheres. Important spectrophotometer optics include the light source intensity, the transmittance of the filters or monochrometers used to select excitation and emission wavelengths, the efficiency of the photomultiplier tube, and the type of reader used (cuvette or microplate). Instrument parameters such as excitation and emission wavelengths and their slit widths will affect the fluorescent signal. On average, we had ~2,600 microspheres/lung piece and obtained an average fluorescent signal of 100.2–212.7 (blue and red, respectively) for the soaking method. Adequate fluorescent signals could have been obtained with many fewer microspheres by simply using wider emission slit widths. Although the fluorescence intensity of a sample can be increased by opening the emission slit width, the “quality” of the signal does not improve, because the signal-to-noise ratio is unchanged.

If the fluorescence intensities of all tissue samples from a given experiment are not measured at the same time, it is important to have fluorescent standards. All the spectrophotometer parameters listed above influence the fluorescent signal obtained from a sample and must remain constant from one run to another. Fluorescent standards, measured before the experimental samples

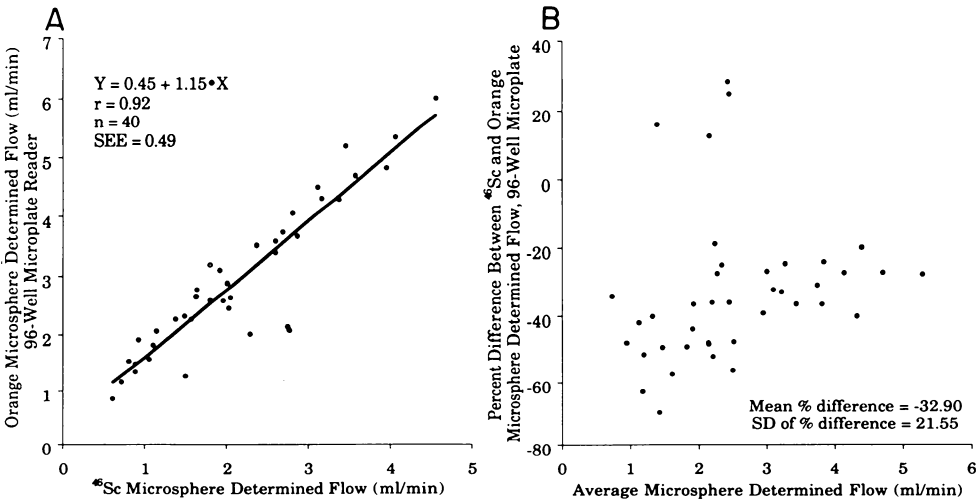


FIG. 8. Regional organ perfusion as determined by simultaneous injection of fluorescent- and radiolabeled microspheres. A: myocardial flow per piece by use of reference flow technique for 1 animal. Five different fluorescent and 3 different radiolabeled microspheres were injected simultaneously. Plot is of 1 fluorescent- and radiolabeled microsphere pair; each point represents 1 tissue piece. Fluorescent dye was extracted from these tissue pieces by filtering method and read in a microplate reader. B: percent difference between regional myocardial perfusion as measured by fluorescent- and radiolabeled microspheres as a function of flow per piece.

TABLE 7. Comparison of myocardial and renal perfusion estimates by use of different microsphere labels

Microsphere Label	Microsphere Label	Organ	r	Slope	Intercept	SEE
Radioactive	Fluorescent	Heart	0.93±0.02	1.13±0.30	0.12±0.13*	0.33±0.15
Radioactive	Fluorescent	Kidney	0.95±0.02	1.03±0.31	0.41±0.18*	0.18±0.06
Fluorescent	Fluorescent	Heart	0.98±0.02	1.06±0.50	-0.01±0.13	0.12±0.03
Fluorescent	Fluorescent	Kidney	0.97±0.00	0.99±0.14	0.02±0.32	0.15±0.03
Radioactive	Radioactive	Heart	1.00±0.00	1.00±0.03	0.02±0.02	0.05±0.01
Radioactive	Radioactive	Kidney	0.99±0.01	1.02±0.04	0.00±0.03	0.10±0.02

Values are means ± SD of 192 myocardial and 120 renal samples. Filtered samples were read in microplates. \* Statistically different from 0.0 ( $P < 0.05$ ).

are run, should be used to verify that all parameters are set appropriately.

The ability to simply soak tissue in solvent compared with digesting and filtering the tissue before addition of solvent is of considerable advantage. Sample handling and hence processing time is greatly decreased. Sample transfer between containers is also decreased, resulting in less chance of error due to loss of microspheres. Unfortunately, the soaking method does not work with dense tissue such as heart and kidney. Attempts to digest these denser tissues with KOH and extract the fluorescent dyes directly from the aqueous solution were not successful because of a large blue signal apparently from collagen. The use of fluorescent microspheres in dense tissue will be greatly enhanced if a faster and cleaner method for extracting the dyes from dense tissue can be found. Despite this problem, the current methods using digestion and filtration work quite well for all colors in solid tissue.

Although estimates of perfusion for samples read in the microplate reader were highly correlated with estimates from radiolabeled microspheres, the microplate reader had some disadvantages compared with the cuvette reader. Radio- and fluorescent-labeled estimates of regional perfusion from microplate readings were less correlated and had slopes farther from unity and intercepts farther from the origin than did the same samples read in cuvettes. The relationship between the number of microspheres and fluorescence intensity was linear over a shorter range with the microplate reader than with the cuvette reader. For some investigators, this amount of error may be acceptable and the disadvantages of the microplate reader may be offset by the greater automation and decreased time and labor requirements.

The time required to process tissue samples depends on the dye extraction method and the type of sample reader. Sample preparation before fluorescent measurement requires 8–10 min for the filtration method and an insignificant amount of time if filtration is not necessary. In addition, when a sample containing six fluorescent colors is read, the fluorescence measurement requires 1 min/sample in cuvettes and 25 s/sample with the microplate reader. The obvious advantage of the microplate reader is that 96 samples can be read without operator assistance.

The only solvents we have evaluated are dimethylformamide, Cellosolve acetate, and xylenes. Dimethylformamide is not an appropriate solvent, because it rapidly degrades some of the fluorescent dyes. Xylenes and Cellosolve acetate both readily dissolve the microspheres

and do not degrade the fluorescent dyes. They both have the disadvantage of being teratogenic and should be used with gloves and within a fume hood. An advantage of Cellosolve acetate over xylenes is that Cellosolve acetate is less volatile and dye concentrations remain constant over many days because of decreased evaporation. After the sample is soaked in solvent for the requisite time, the fluorescence of each sample should be read promptly to decrease any error due to evaporation. An advantage of xylenes over Cellosolve acetate is that xylenes produce a much narrower emission spectrum in the blue range of colors.

Whereas all the fluorescent measurements in this study were made at specific pairs of excitation and emission wavelengths, measurements can also be obtained using a synchronous scanning method. During a synchronous scan, the separation between excitation and emission wavelengths ( $\Delta\lambda$ ) is fixed and is roughly equal to the Stokes shift of the fluorescent signals of interest. The exciting light then sweeps through the entire spectrum, generating an output curve of the fluorescence intensity at (excitation wavelength +  $\Delta\lambda$ ) as a function of excitation wavelength. The peak intensities for each color can be used to estimate deposition of microspheres. The principal advantages of this method are its speed and simplicity. The disadvantage is some loss of fluorescent signal. As shown in Table 1, the optimal range for  $\Delta\lambda$  is 20–48 nm. Because  $\Delta\lambda$  is fixed during a synchronous scan, the optimal excitation/emission pairings are not used. However, if the same  $\Delta\lambda$  is used when all tissue samples are scanned, the signal loss will be consistent and the fluorescence intensity will provide a relative measure of microsphere deposition. An optimal  $\Delta\lambda$  for the fluorescent colors used in this study is 20 nm.

The costs associated with automated radiolabeled, fluorescent-labeled, and color microsphere methods are different enough to warrant mention. All reported costs are those quoted by each company as of May 1992 and include the computer and software needed to run the specific instrument (Table 8). The cost of radiolabeled microspheres depends on the particular radiolabel and its activity. The two methods available for quantitating colored microsphere deposition are a computer-driven fluorescent microscope and an ultraviolet-visible spectrophotometer (13). Alternatively, tissue samples with colored microspheres can be read by E-Z Trac for \$10–22.50/sample (depending on quantity). Material costs per experiment (excluding instrument purchase) are dependent on the number of microspheres needed per tissue sample to produce an adequate signal and appear to be within simi-

TABLE 8. Cost comparisons of automated microsphere quantitation methods

Item	Microsphere Label			X-Ray Fluorescence
	Radioactive	Colored	Fluorescent	
Microspheres <i>n</i>	\$200–1,000 10 × 10 <sup>6</sup> (NEN Research)	\$225 100 × 10 <sup>6</sup> (EZ-Trac)	\$110 10 × 10 <sup>6</sup> (Molecular Probes)	\$75 100 × 10 <sup>6</sup> (Sekisui)
Instrument	\$27,000 (model M5530B2, Packard)	\$9,000 (model 8452A, Hewlett-Packard) \$34,995 (model 600-100, EZ-Trac)	\$24,000 (model LS-50, Perkin-Elmer)	\$220,000 (model PW 1480, Philips)
Filters	NA	\$30/100	\$30/100	\$30/100
Disposal	\$13.26/kg (Hanford Nuclear Facility, WA)	None	None	None

lar ranges for each of the methods. Additional costs associated with radiolabeled microsphere include disposal of radioactive material, which is currently quite expensive and will likely become considerably more costly. Another advantage of colored and fluorescent-labeled microspheres over radiolabeled microspheres is the extended shelf life. The manufacturer of our fluorescent-labeled microspheres claims a shelf life of 2 yr, which compares favorably with radiolabeled microspheres, which have a limited shelf life because of radioactive decay. If cost is an important consideration, both the colored and fluorescent-labeled microspheres can be used with a light or epifluorescence microscope and a counting chamber to estimate regional organ perfusion (8, 12). The personnel costs for processing samples are not included in Table 8 but are likely considerably more for the fluorescent-labeled and colored microspheres because of the time needed to filter tissues.

This study is the initial attempt at validating the use of fluorescent-labeled microspheres for measuring regional organ perfusion and, as such, introduces relatively primitive methodologies. When first introduced by Rudolf and Heyman (15), radiolabeled microsphere methods were similarly rudimentary. It is hoped that fluorescent-labeled microsphere techniques will evolve in an analogous fashion. Although promissory, there are a number of potential improvements to the methods we have presented. Theoretically, the excitation and emission slit widths should be increased to 8 and 6 nm, respectively, resulting in a threefold increase in the fluorescent signal with little change in spillover. With this increased signal, larger volumes of solvent can be used for each sample, reducing the error from unequal volumes. The manufacturer of our microspheres will soon offer a total of 10–12 fluorescent colors. Because these colors will be more closely spaced, correction for spillover will become necessary. Deconvolution software already exists commercially for separating multiple overlapping infrared and ultraviolet spectra. Such software requires that a synchronous scanning mode be used, which will in turn increase the rate at which samples can be read. The available deconvolution software also corrects for any nonlinearity within the fluorescent method, which should make the 96-well plate reader a more viable method. The greatest room for improvement is in sample processing. Methods using centrifugation filtering are currently being evaluated that should greatly facilitate the preprocessing of solid organ

tissues. These new methods will allow many samples to be filtered at the same time and circumvent the need to transfer samples between containers.

We thank Dowon An, Sarah Levy, Dr. Irving Shen, and Sharon Bradley for technical assistance.

This work was supported by grants from the American Lung Association and National Heart, Lung, and Blood Institute Grants HL-02625 and HL-47687.

Address for reprint requests: R. W. Glenny, Div. of Pulmonary and Critical Care Medicine, University of Washington, RM-12, Seattle, WA 98196.

Received 24 July 1992; accepted in final form 10 November 1992.

## REFERENCES

1. AUSTIN, R. E., W. W. HAUCK, G. S. ALSEA, A. E. FLYNN, D. L. COGGINS, AND J. I. E. HOFFMAN. Quantitating error in blood flow measurements with radioactive microspheres. *Am. J. Physiol.* 257 (*Heart Circ. Physiol.* 26): H280–H288, 1989.
2. BAER, R. W., B. D. PAYNE, E. D. VERRIER, G. J. VLAHAKES, D. MOLODOWITZ, P. N. UHLIG, AND J. I. E. HOFFMAN. Increased number of myocardial blood flow measurements with radionuclide-labeled microspheres. *Am. J. Physiol.* 246 (*Heart Circ. Physiol.* 15): H418–H434, 1984.
3. BASSINGTHWAIGHTE, J. B., M. A. MALONE, T. C. MOFFETT, R. B. KING, S. E. LITTLE, J. M. LINK, AND K. A. KROHN. Validity of microsphere deposition for regional myocardial flows. *Am. J. Physiol.* 253 (*Heart Circ. Physiol.* 22): H184–H193, 1987.
4. BLAND, J. M., AND D. G. ALTMAN. Statistical methods for assessing agreement between two methods of clinical measurement. *Lancet* 1: 307–310, 1986.
5. BUCKBERG, G. D., J. C. LUCK, D. B. PAYNE, J. I. E. HOFFMAN, J. P. ARCHIE, AND D. E. FIXLER. Some sources of error in measuring regional blood flow with radioactive microspheres. *J. Appl. Physiol.* 31: 598–604, 1971.
6. GOTTLIEB, G. J., S. H. KUBO, AND D. R. ALONSO. Ultrastructural characterization of the border zone surrounding early experimental myocardial infarcts in dogs. *Am. J. Pathol.* 103: 292–303, 1981.
7. GUILBAULT, G. G. Practical fluorescence. In: *Modern Monographs in Analytical Chemistry*, edited by G. G. Guilbault. New York: Dekker, 1990, vol. 3.
8. HALE, S. L., K. J. ALKER, AND R. A. KLONER. Evaluation of nonradioactive, colored microspheres for measurement of regional myocardial blood flow in dogs. *Circulation* 78: 428–434, 1988.
9. HALE, S. L., M. T. VIVALDI, AND R. A. KLONER. Fluorescent microspheres: a new tool for visualization of ischemic myocardium in rats. *Am. J. Physiol.* 251 (*Heart Circ. Physiol.* 20): H863–H868, 1986.
10. HEYMAN, M. A., B. D. PAYNE, J. I. HOFFMAN, AND A. M. RUDOLF. Blood flow measurements with radionuclide-labeled particles. *Prog. Cardiovasc. Dis.* 20: 55–79, 1977.
11. JASPER, M. S., P. McDERMOTT, D. S. GANN, AND W. C. ENGLAND. Measurement of blood flow to the adrenal capsule, cortex

- and medulla in dogs after hemorrhage by fluorescent microspheres. *J. Auton. Nerv. Syst.* 30: 159-168, 1990.
12. KINOSHITA, K., D. J. HEARSE, M. V. BRAIMBRIDGE, AND A. S. MANNING. "Early" ischemia and reperfusion-induced arrhythmias: antiarrhythmic effects of diltiazem in the conscious rat. *Can. J. Cardiol.* 4: 37-43, 1988.
  13. KOWALLIK, P., R. SCHULZ, B. D. GUTH, A. SCHADE, W. PAFFHAUSEN, R. GROSS, AND G. HEUSCH. Measurement of regional myocardial blood flow with multiple colored microspheres. *Circulation* 83: 974-982, 1991.
  14. MORI, H., S. HARUYAMA, Y. SHINOZAKI, H. OKINO, A. IIDA, R. TAKANASHI, I. SAKUMA, W. K. HUSSEINI, B. D. PAYNE, AND J. I. E. HOFFMAN. New nonradioactive microspheres and more sensitive X-ray fluorescence to measure regional blood flow. *Am. J. Physiol.* 263 (*Heart Circ. Physiol.* 32): H1946-H1957, 1992.
  15. RUDOLF, A. M., AND M. A. HEYMAN. The circulation of the fetus in utero: methods for studying distribution of blood flow, cardiac output and organ blood flow. *Circ. Res.* 21: 163-184, 1967.
  16. SCHOSSER, R., K. E. ARFORS, AND K. MESSMER. MIC-II—a program for the determination of cardiac output, arterio-venous shunt and regional blood flow using the radioactive microsphere method. *Comp. Prog. Biomed. Res.* 9: 19-38, 1979.
  17. WESTGARD, J. O., AND M. R. HUNT. Use and interpretation of common statistical tests in method-comparison studies. *Clin. Chem.* 19: 49-57, 1973.
  18. YEN, R. T., AND Y. C. FUNG. Effect of velocity distribution on red cell distribution in capillary blood vessels. *Am. J. Physiol.* 235 (*Heart Circ. Physiol.* 4): H251-H257, 1978.
  19. ZWISSLER, B., R. SCHOSSER, C. WEISS, V. IBER, M. WEISS, C. SCHWICKER, P. SPENGLER, AND K. MESSMER. Methodologic error and spatial variability of organ blood flow measurements using radiolabeled microspheres. *Res. Exp. Med.* 191: 47-63, 1991.

